
ALGORITHMIC COMPLIANCE AND REGULATORY LOSS IN DIGITAL ASSETS

A PREPRINT

Khem Raj Bhatt
Krishna Sharma

ABSTRACT

We study the deployment performance of machine learning–based enforcement systems used in cryptocurrency anti-money laundering (AML). Using forward-looking and rolling evaluations on Bitcoin transaction data, we show that strong static classification metrics substantially overstate real-world regulatory effectiveness. Temporal non-stationarity induces pronounced instability in cost-sensitive enforcement thresholds, generating large and persistent excess regulatory losses relative to dynamically optimal benchmarks. The core failure arises from miscalibration of decision rules rather than from declining predictive accuracy per se. These findings underscore the fragility of fixed AML enforcement policies in evolving digital asset markets and motivate loss-based evaluation frameworks for regulatory oversight.

Keywords: Cryptocurrency, Anti-Money Laundering, Concept Drift, Regulatory Technology, Model Risk

1 Introduction

The rapid expansion of cryptocurrency markets has intensified regulatory concern over illicit financial activity conducted through digital assets. Empirical evidence using Bitcoin transaction data suggests that illegal activity has accounted for a substantial share of on-chain usage in some periods, particularly linked to darknet-market flows (Foley et al., 2019). In response, regulators, exchanges, and blockchain analytics firms increasingly rely on automated anti-money laundering (AML) systems to monitor transactions at scale. These systems are typically evaluated using static classification metrics such as the area under the receiver operating characteristic curve (ROC-AUC) or the precision-recall area under the curve (PR-AUC). While such metrics summarize ranking performance, they abstract from the decision environment in which AML systems actually operate.

In practice, regulators must select enforcement thresholds that determine which transactions are flagged for investigation. These thresholds reflect asymmetric costs: false negatives allow illicit activity to proceed, while false positives generate investigative burden and compliance costs. As emphasized in the cost-sensitive decision-making literature, optimal classification depends not only on predictive accuracy but also on how misclassification costs enter downstream enforcement decisions (Elkan, 2001). Industry accounts of transaction monitoring reinforce that alert volumes, false-positive rates, and threshold governance are first-order operational constraints in AML programs (Oztas et al., 2024). Supervisory expectations have similarly become more explicit: Financial Action Task Force’s (FATF) risk-based guidance for virtual assets and Virtual Asset Service Providers (VASP) emphasizes ongoing risk assessment and monitoring, with controls calibrated to evolving typologies and risk exposure (Force, 2021). Together, these perspectives underscore that AML performance is ultimately determined by how model outputs are translated into enforcement actions, not by ranking accuracy alone.

Yet most empirical evaluations of AML systems implicitly assume stationarity: models are trained and tested as if the underlying data-generating process and the associated optimal enforcement threshold remain stable over time. This assumption is particularly problematic in cryptocurrency markets, where prior work finds that Bitcoin often behaves more like a speculative asset than a medium of exchange and that its pricing dynamics can vary substantially across market conditions, implying that relationships estimated in one period may not remain stable out of sample (Baek and Elbeck, 2015; Baur et al., 2018; Biais et al., 2023). When feature distributions, label frequencies, or their joint relationship evolve, models trained on historical data may become systematically misaligned with current conditions (Widmer and Kubat, 1996; Gama et al., 2014). Crucially, this misalignment need not manifest as declining predictive accuracy. The model risk literature emphasizes that decisions calibrated in one regime can become unreliable as conditions shift (Danielsson et al., 2016). In our empirical setting, we show that strong static classification performance can co-exist with large deployment losses because fixed enforcement thresholds become miscalibrated as class prevalence and score distributions evolve over time.

This paper addresses that gap by studying the deployment performance of automated AML systems in an evolving crypto transaction network. Using the Elliptic Bitcoin transaction dataset, we move beyond static evaluation and implement forward-looking and rolling deployment designs that more closely mirror real-world regulatory use. We explicitly model regulatory loss as a function of false positives and false negatives and examine how cost-sensitive enforcement thresholds evolve over time. This framework allows us to quantify the economic cost of deploying static decision rules in a non-stationary environment, relative to an infeasible but informative oracle benchmark that re-optimizes thresholds ex-post. We summarize this inefficiency using the deployment gap, defined as realized loss under the historically calibrated threshold minus the oracle loss under contemporaneous re-optimization. Regulatory fragility therefore arises not primarily from declining predictive accuracy, but from miscalibration of decision rules as market conditions and illicit prevalence evolve.

Our results reveal a clear disconnect between static classification performance and realized regulatory outcomes. Random train-test splits suggest strong predictive accuracy, but forward and rolling evaluations uncover pronounced instability in optimal enforcement thresholds and large, persistent excess regulatory losses. These losses are economically

meaningful and robust across regulatory cost ratios, often approaching or exceeding a doubling of loss relative to the oracle benchmark. We employ a simple and transparent predictive model to isolate the role of deployment design and regulatory decision rules from model-specific effects. By focusing on deployment loss rather than statistical accuracy alone, this paper contributes to three strands of literature. First, we complement research on concept drift by documenting its economic consequences in a regulatory context. Second, we add to the financial machine learning and model risk literature by showing how conventional evaluation practices can mask deployment fragility. Third, we contribute to the literature on cryptocurrency regulation and regulatory technology by reframing AML effectiveness in terms of loss-based outcomes rather than static classification metrics (Anagnostopoulos, 2018; Hardjono et al., 2021).

The remainder of the paper proceeds as follows. Section 2 reviews the related literature. Section 3 describes the data and institutional setting. Section 4 outlines the regulatory decision framework. Section 5 presents the empirical results. Section 6 discusses policy implications and limitations. Section 7 concludes.

2 Related Literature

This paper relates to four strands of literature: the economics of cryptocurrencies and regulatory technology; model risk in financial decision systems; classifier evaluation and cost-sensitive decision making; and learning under non-stationarity. Our contribution lies in linking these strands through an explicit focus on the economic performance of deployed regulatory decision rules. While cost-sensitive and adaptive detection approaches exist, deployment-centered evidence on the regulatory loss consequences of holding enforcement thresholds fixed under temporal non-stationarity remains limited.

A first strand concerns the regulation of digital asset markets and the feasibility of transaction monitoring. Anagnostopoulos (2018) and Hardjono et al. (2021) propose infrastructure for VASP-facing compliance (e.g., identity/key management), highlighting implementation challenges for secure VA ecosystems. Foley et al. (2019) estimate that a substantial share of cryptocurrency transactions has historically been associated with illicit activity, underscoring the importance of effective AML systems. Using heuristic clustering on the public ledger, Meiklejohn et al. (2013) demonstrate that transaction graphs can link clusters of activity to real-world services, providing a foundation for compliance analytics. Weber et al. (2019) introduce the Elliptic dataset and benchmark supervised methods for illicit transaction classification, while Schnoering and Vazirgiannis (2025) large-scale temporally annotated Bitcoin transaction graphs for broader blockchain analytics. More recent theoretical contributions model Bitcoin pricing (Biais et al., 2023) and token-based platform finance (Cong et al., 2022), highlighting how incentives and market structure can shape outcomes in tokenized ecosystems. Early empirical work documents that Bitcoin exhibits strong speculative components and time-varying market behavior (Baek and Elbeck, 2015; Baur et al., 2018), while evidence such as the Kimchi premium highlights market frictions and speculative trading that can vary across venues and over time (Eom, 2021). In addition, evidence of coordinated price manipulation episodes suggests that crypto markets can experience abrupt shifts in behavior that complicate stable inference (Gandal et al., 2018). These dynamics imply that the statistical properties of transaction data, including illicit prevalence and observable transaction patterns, may vary substantially over time.

A second strand applies machine learning methods to financial data, with particular attention to model risk and evaluation design. Gu et al. (2020) and Kelly et al. (2019) show that high-dimensional predictors/ML methods can be competitive in asset pricing tasks, while Sirignano and Cont (2021) document stable patterns in price formation using deep learning. At the same time, Bailey et al. (2017) show that back-test overfitting is pervasive in financial applications, and De Prado (2018) emphasize the importance of robust validation and deployment practices. Danielsson et al. (2016) formalize model risk and show that decisions calibrated in one regime may become unreliable as conditions shift. We complement this literature by showing that even simple, well-performing classifiers can generate substantial regulatory losses when cost-sensitive decision rules are not dynamically recalibrated.

A third strand concerns how predictive models are evaluated and translated into operational decisions. As class prevalence shifts, conventional ranking summaries can give a distorted picture of operational performance: ROC-based measures may appear stable even when precision and PR performance change materially, because the ROC-PR relationship depends directly on the base rate (Fawcett, 2006; Hand, 2009; Davis and Goadrich, 2006). Saito and Rehmsmeier (2015) further show that precision-recall summaries are often more informative than ROC-based summaries under severe class imbalance, which closely matches AML settings. More fundamentally, Elkan (2001) demonstrates that optimal classification depends on asymmetric misclassification costs rather than statistical accuracy alone, and Nami and Shajari (2018) develop cost-sensitive fraud detection methods that embed these costs directly into the detection objective. Kleinberg et al. (2016) and Corbett-Davies et al. (2023) further show that trade-offs between competing objectives are inherent in risk-scoring systems, and that mismeasurement arises when ranking performance is conflated with decision quality. Davis and Goadrich (2006) link precision-recall and ROC curves and emphasize that metric choice materially affects perceived performance under class imbalance. Building on these insights, we examine how cost-sensitive enforcement thresholds evolve over time and show that static deployment rules can generate economically meaningful losses in non-stationary environments.

A fourth strand studies predictive modeling when the data-generating process evolves. Widmer and Kubat (1996) formalize learning under concept drift, emphasizing that models trained on historical data may become systematically misaligned as underlying patterns change. Gama et al. (2014) survey concept drift adaptation methods and highlight a fundamental trade-off between stability and adaptability in deployed systems. Moreno-Torres et al. (2012) provide a unifying framework for distinguish changes in covariates, class priors, and the conditional relationship between features and labels across training vs deployment. Recent work also proposes graph neural network architectures for blockchain fraud detection (Haider et al., 2025). However, even dynamic modeling approaches do not by themselves resolve the governance problem of deploying cost-sensitive decision rules under drift. Our analysis extends this literature by quantifying the regulatory costs of failing to adapt enforcement thresholds in a rapidly evolving market environment.

3 Institutional Setting and Data

3.1 Institutional Context: Automated AML in Crypto Markets

Cryptocurrency exchanges and virtual asset service providers are subject to AML obligations analogous to those imposed on traditional financial institutions. In practice, compliance is operationalized through automated risk-scoring systems that assign a probability of illicit activity to each transaction and trigger enforcement actions when scores exceed a pre-specified threshold. Such systems implement a resource allocation rule under asymmetric costs. Compliance teams face regulatory penalties for under-enforcement, operational costs from over-enforcement, and capacity constraints in investigative review. The performance of an AML system is therefore not defined solely by predictive accuracy, but by how effectively it minimizes regulatory loss given these constraints. Our empirical setting mirrors this regulatory deployment problem using transaction-level data from the Bitcoin network.

3.2 Data Source and Sample Construction

We use the publicly available Elliptic Bitcoin transaction dataset, which has become a benchmark for studying illicit cryptocurrency activity (Weber et al., 2019). Its structure combines transaction-level labels with a time-indexed transaction graph, making it well suited for analyzing how predictive systems perform when deployed sequentially over time.

The dataset offers two key advantages for our purposes. First, it contains transaction-level labels informed by proprietary heuristics and law enforcement intelligence, allowing us to approximate the ground truth used in real-world AML monitoring. While these labels are necessarily imperfect, they reflect the practical reality of AML enforcement,

in which compliance decisions rely on noisy ground truth constructed from investigations and heuristic rules rather than definitive ex-post verification. Second, the dataset’s discrete temporal structure permits forward-looking and rolling evaluation designs that closely mirror actual deployment conditions.

The dataset consists of a directed transaction graph in which nodes represent Bitcoin transactions and edges represent flows of funds. Each transaction is assigned a discrete time index from 1 to 49. Transactions are labeled as either illicit or licit based on Elliptic’s classification procedures. Observations labeled as unknown are excluded from the analysis. After excluding unlabeled observations, the final sample contains 46,564 labeled transactions, of which 9.8 percent are illicit. Illicit prevalence declines over time, falling from 14.3 percent in early periods to 5.3 percent in later periods. This time variation in the base rate of illicit activity is economically meaningful because optimal cost-sensitive enforcement thresholds depend mechanically on both predicted risk scores and class prevalence. As a result, shifts in illicit incidence directly affect the regulatory loss associated with fixed enforcement rules. These descriptive dynamics are summarized in Appendix A, Table A1.

3.3 Features and Information Structure

Each transaction is described by 165 engineered features capturing transaction behavior, local network structure, and aggregate flow characteristics. All features are constructed using information available at or before each transaction’s time step. No forward-looking information is used in model training or evaluation, preventing look-ahead bias. These features approximate the information set available to blockchain analytics firms and compliance teams at the time of monitoring.

3.4 Empirical Implementation

We exclude observations labeled *unknown* and restrict attention to transactions with definitive licit or illicit labels. Transactions are indexed by discrete time steps $t \in \{1, \dots, 49\}$, and all evaluation designs enforce temporal ordering.

Predicted illicit risk is generated using a regularized logistic regression classifier with L2 penalization. Features are standardized using training-sample moments, and the same transformation is applied to the corresponding test data. We report three evaluation protocols. (i) A random split benchmark using a stratified 70/30 split that ignores temporal ordering and serves only as a conventional baseline. (ii) A forward split that trains on transactions with $t \leq 34$ and tests on transactions with $t \geq 35$. (iii) A rolling deployment design in which, for each test period t , the classifier is trained on the preceding 10 time steps $\{t - 10, \dots, t - 1\}$ and deployed on transactions observed at t ; periods with fewer than 50 labeled test transactions are excluded to avoid unstable period-level metrics.

Enforcement thresholds are chosen to minimize the cost-sensitive regulatory loss function described in Section 4. In the forward and rolling designs, the loss-minimizing threshold τ^* is selected using training data only and then held fixed when computing test outcomes. For benchmarking purposes, we also compute an infeasible oracle that re-optimizes τ^* using contemporaneous test data; the oracle is not deployable and serves only to benchmark the cost of holding thresholds fixed under temporal non-stationarity. Regulatory loss is computed in levels as $C_{FN} \times FN + C_{FP} \times FP$ within each test period. Because rolling outcomes are serially correlated across adjacent test periods, uncertainty in average deployment loss and excess loss is assessed using a moving block bootstrap over contiguous test periods, with block lengths 3, 5, and 7 and 5,000 bootstrap replications.

4 Empirical Framework: Regulatory Loss under Deployment

4.1 Automated AML as a Regulatory Decision Problem

We conceptualize automated AML systems as implementing a regulatory decision rule rather than a purely predictive task. At each point in time, transactions generate observable signals summarized by model-based risk scores that reg-

ulators or compliance teams must translate into enforcement actions through an enforcement threshold that determines which transactions are flagged for investigation, delayed, or blocked.

The enforcement threshold is a policy instrument chosen under asymmetric costs and operational constraints. False negatives allow illicit activity to proceed and may generate regulatory penalties or reputational harm, while false positives impose investigative burdens, compliance costs, and potential disruption to legitimate users. Given limited investigative capacity, the regulator’s objective is not to maximize predictive accuracy, but to minimize expected regulatory loss. The loss-minimizing enforcement threshold depends on three objects: (i) the distribution of risk scores produced by the model, (ii) the underlying prevalence of illicit activity, and (iii) the relative costs of false positives and false negatives. Even when the predictive model itself remains fixed, changes in any of these objects alter the optimal decision rule. In non-stationary environments, the optimal enforcement threshold is therefore inherently time-varying.

Regulatory fragility arises when enforcement thresholds calibrated under past conditions are deployed in evolving environments. When transaction patterns, illicit prevalence, or score distributions shift, static thresholds become misaligned with current conditions, generating excess regulatory loss even when conventional measures of predictive performance, such as ROC-AUC or PR-AUC, remain high. By comparing realized regulatory loss under historically calibrated thresholds to an infeasible benchmark that re-optimizes thresholds ex-post, we isolate the economic cost of static decision rules in a non-stationary environment.

4.2 Regulatory Objective

We model automated AML systems as implementing a cost-minimizing regulatory policy. Let $y_i \in \{0, 1\}$ denote the true status of transaction i , where $y_i = 1$ indicates illicit activity, and let \hat{p}_i denote the predicted probability that transaction i is illicit. A transaction is flagged if $\hat{p}_i \geq \tau$, where τ is an enforcement threshold.

Following Elkan (2001), regulatory loss is defined as:

$$L(\tau) = C_{FN} \cdot FN(\tau) + C_{FP} \cdot FP(\tau),$$

where $FN(\tau)$ and $FP(\tau)$ denote the number of false negatives and false positives induced by threshold τ , and C_{FN} and C_{FP} represent the relative costs of these errors. This loss function captures regulatory penalties, reputational damage, compliance costs, and investigative burdens. Cost-sensitive objectives are common in fraud detection research and are often implemented by weighting false negatives more heavily than false positives (Nami and Shajari, 2018). In AML settings, thresholds are tuned to manage alert volumes under binding investigative capacity, making the economic relevance of false positives and false negatives inherently operational (Oztas et al., 2024). The regulator’s objective is to choose the enforcement threshold τ that minimizes expected loss.

We evaluate regulatory loss under two alternative cost ratios, $C_{FN}/C_{FP} \in \{10, 25\}$. These values are not intended to represent precise or estimated regulatory parameters, which are rarely observable in practice, but rather to capture economically plausible asymmetry between the costs of false negatives and false positives in AML enforcement. The cost-sensitive learning literature emphasizes that enforcement objectives in high-risk environments typically place far greater weight on avoiding false negatives than on minimizing routine compliance costs (Elkan, 2001), and the model risk literature highlights that decision-rule miscalibration under changing environments can amplify losses even when predictive accuracy appears stable (Danielsson et al., 2016). We therefore use moderate and high penalty ratios to assess whether deployment fragility persists across alternative but economically relevant enforcement environments. All core results are reported under both cost ratios, providing a sensitivity analysis with respect to the relative cost of misclassification. Supplementary evidence, including rolling-window summaries and block bootstrap inference under alternative dependence assumptions, is reported in Appendix A and Appendix B.

4.3 Enforcement Thresholds, Deployment Design, and Evaluation

We treat enforcement thresholds as policy instruments rather than as mechanical outputs of predictive models. The loss-minimizing threshold depends on three objects that may all evolve over time: the distribution of predicted risk scores, the underlying prevalence of illicit activity, and the relative costs of false positives and false negatives. As a result, regulatory fragility can arise through threshold miscalibration even when the underlying predictive model remains fixed and continues to exhibit strong ranking performance.

We compare three evaluation regimes. First, a conventional random train-test split assumes stationarity and provides a benchmark comparable to much of the existing machine learning literature. Second, a forward split trains the model on early periods and evaluates it on later periods, approximating real-world regulatory rollout while eliminating temporal leakage. Third, we implement a rolling deployment design in which, at each time step t , the model is trained on a fixed-length historical window ending at $t - 1$ and deployed on transactions observed at t . In this design, the enforcement threshold is optimized using training data only and then held fixed during deployment, mirroring operational AML systems where retraining and recalibration are costly and therefore infrequent.

To isolate the inefficiency arising from static threshold deployment, we construct an infeasible oracle benchmark that re-optimizes the enforcement threshold using contemporaneous test data. Let L_t^{deploy} denote regulatory loss under the historically calibrated threshold and L_t^{oracle} denote loss under the oracle threshold. We define excess regulatory loss as

$$\text{Excess Loss}_t = L_t^{deploy} - L_t^{oracle}.$$

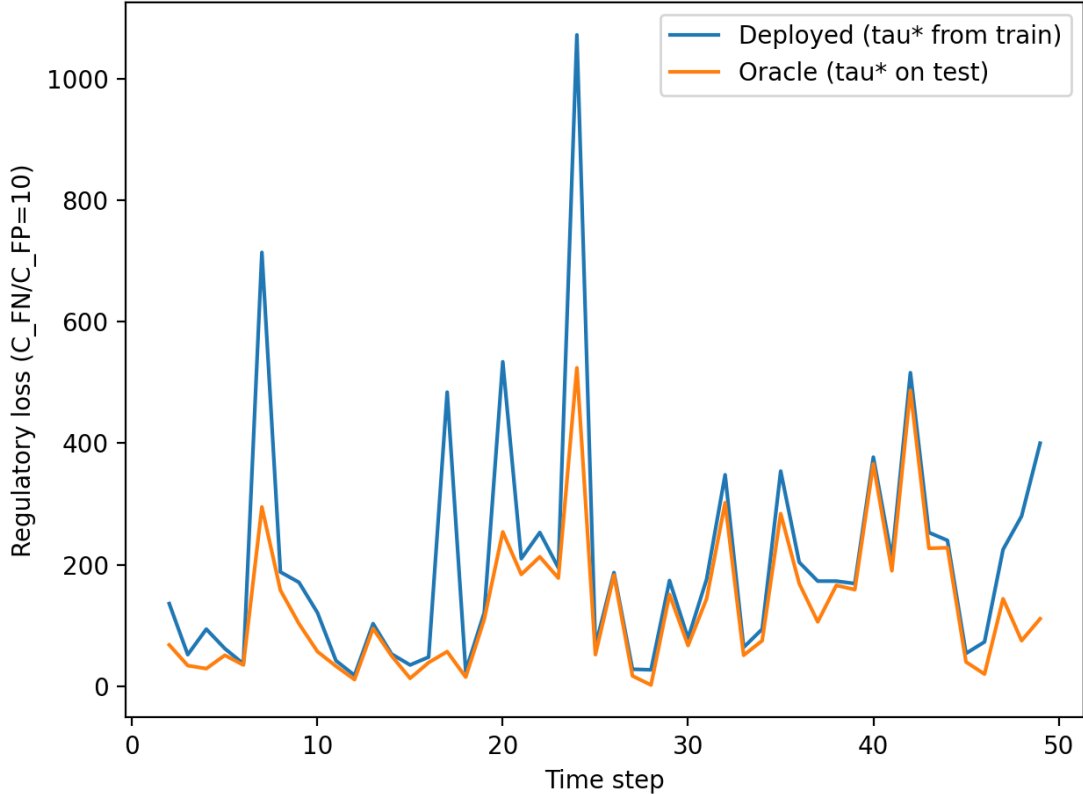
This quantity provides a direct measure of regulatory inefficiency attributable to threshold miscalibration in a changing environment, holding the predictive model fixed. For comparability with prior work, we also report standard classification metrics, including ROC-AUC and PR-AUC (Fawcett, 2006; Hand, 2009). However, our primary outcomes are economic rather than statistical: realized regulatory loss, excess regulatory loss relative to the oracle benchmark, deployment-to-oracle loss ratios, and precision among the highest-risk transactions.

5 Results

We begin by evaluating regulatory performance under deployment, comparing enforcement thresholds calibrated on historical data to an infeasible oracle benchmark that re-optimizes thresholds using contemporaneous information. Figures 1 and 2 plot realized regulatory loss over time under two alternative cost ratios, $C_{FN}/C_{FP} \in \{10, 25\}$, which serve as distinct but economically plausible enforcement environments rather than calibrated policy parameters.

Across both cost ratios, deployed regulatory loss systematically exceeds oracle loss. Importantly, the deployment gap is highly time-varying. Loss differentials widen sharply during periods of market transition and contract during relatively stable intervals, indicating that excess regulatory loss is state-dependent rather than a mechanical artifact of model choice or evaluation design. Appendix A, Figures A3 and A4 plot the deployed-to-oracle loss ratio over time, confirming that deployment inefficiency is episodic rather than uniform. Under $C_{FN}/C_{FP} = 10$ (Figure 1), deployed loss frequently approaches or exceeds twice the oracle benchmark during transition periods. When the relative cost of false negatives is increased to $C_{FN}/C_{FP} = 25$ (Figure 2), loss spikes become larger and more persistent, reflecting the heightened sensitivity of enforcement outcomes to threshold miscalibration when under-enforcement is more costly.

Table 1 summarizes the magnitude of this deployment gap across rolling windows. Mean deployed loss exceeds oracle loss by approximately 69 units under $C_{FN}/C_{FP} = 10$ and by 154 units under $C_{FN}/C_{FP} = 25$. These average effects mask substantial episodic instability. The aggregate ratio of means (1.51 and 1.75) understates the magnitude of inefficiency observed during peak periods. Mean window-level loss ratios of 1.97 and 2.23 indicate that the average rolling test window incurs approximately 97 and 123 percent more regulatory loss than the oracle benchmark, respectively, with short-lived but severe spikes accounting for a large share of overall deployment loss. The dispersion and right tail of these loss spikes is summarized in Appendix A, Figure A2. Moving block bootstrap confidence intervals

Figure 1: Regulatory loss over time ($C_{FN}/C_{FP} = 10$).

exclude zero excess loss across alternative block lengths, confirming that these patterns are statistically robust rather than driven by sampling noise. Full moving-block bootstrap results across alternative block lengths are reported in Appendix A, Table A3.

Table 1: Deployment Gap: Deployed versus Oracle Regulatory Loss

Cost Ratio	Mean Deployed	Mean Oracle	Ratio (Means)	Mean Window Ratio	Mean Excess Loss
$C_{FN}/C_{FP} = 10$	202.33	133.79	1.51	1.97	68.54
$C_{FN}/C_{FP} = 25$	359.58	205.33	1.75	2.23	154.25

To understand the source of this deployment fragility, we examine the evolution of the loss-minimizing enforcement threshold over time. Figure 3 plots the optimal threshold τ^* estimated on rolling training windows for $C_{FN}/C_{FP} = 10$. The threshold exhibits pronounced instability, including discrete jumps and sustained drift across adjacent periods, despite the predictive model itself being held fixed. Appendix B, Figures B5 and B6 visualize the deployed-versus-oracle threshold miscalibration gap directly.

This instability follows mechanically from the regulatory loss function. For a fixed cost ratio, the loss-minimizing threshold depends on both the prevalence of illicit activity and the distribution of predicted risk scores. Changes in either object alter the trade-off between false positives and false negatives, shifting the optimal enforcement rule even when predictive accuracy remains stable. As shown in Appendix A (Figure A1), illicit prevalence declines markedly over time in the rolling test windows. Periods of sharp base-rate decline coincide with downward adjustments in the optimal threshold, as the marginal cost of false positives rises relative to false negatives. Conversely, periods of

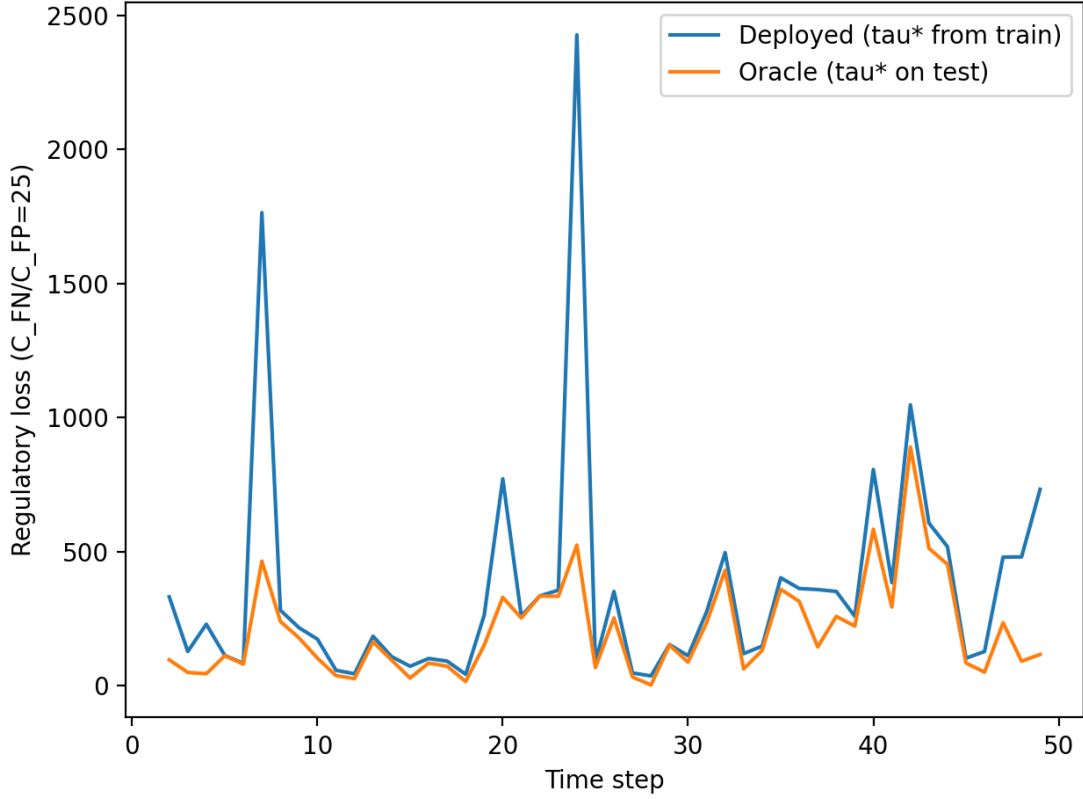


Figure 2: Regulatory loss over time ($C_{FN}/C_{FP} = 25$).

elevated or stabilizing illicit prevalence are associated with higher and more stable thresholds, consistent with the threshold jumps observed in Figure 3.

In parallel, shifts in the distribution of predicted risk scores contribute to threshold instability. As score distributions compress or shift over time, reflecting changes in transaction behavior and network structure, the same nominal threshold corresponds to different effective false-positive and false-negative rates. Consistent with this mechanism, periods characterized by greater score dispersion are associated with higher loss-minimizing thresholds and lower deployment loss, whereas compressed score distributions coincide with threshold drops and loss spikes.

Table 2 summarizes these relationships using rolling-window averages. Windows with lower illicit prevalence and compressed score distributions exhibit systematically lower thresholds and higher deployed-to-oracle loss ratios. These patterns arise directly from the structure of the regulatory loss function under temporal non-stationarity and require no additional estimation. A quantitative summary of deployment loss by illicit prevalence tertile is reported in Appendix B, Table B5. Supplementary descriptive evidence on base-rate dynamics and rolling-window summaries is reported in Appendix A (Figure A1; Table A2), and the distribution of deployment loss ratios is shown in Appendix A, Figure A2.

Table 2: Mechanism Summary: Base Rates, Thresholds, and Deployment Loss

Rolling Window Characteristic	Mean Illicit Share	Mean τ_{train}^*	Mean Loss Ratio
High illicit prevalence windows	High	Higher	Lower
Low illicit prevalence windows	Low	Lower	Higher

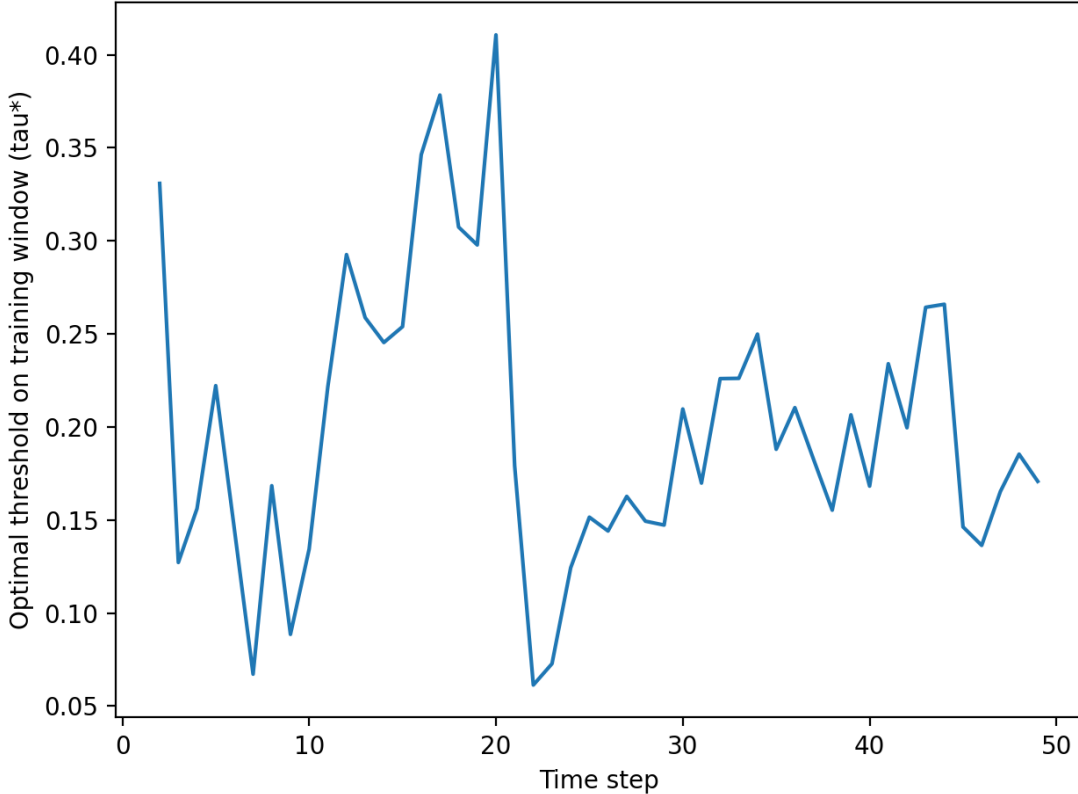


Figure 3: Optimal threshold τ^* over time ($C_{FN}/C_{FP} = 10$).

Finally, we contrast these deployment outcomes with conventional static evaluation. Table 3 compares a random train-test split to a forward, time-respecting split. Under random sampling, the classifier appears highly effective, with PR-AUC of 0.77, ROC-AUC exceeding 0.96, and top-one-percent precision above 0.82. Once temporal ordering is respected, performance deteriorates sharply. PR-AUC falls to 0.36, top-one-percent precision declines to 0.43, and test loss nearly doubles under both cost ratios.

Table 3: Random versus Forward Evaluation Performance

Protocol	C_{FN}/C_{FP}	PR-AUC	ROC-AUC	τ_{train}^*	Test Loss	Top 1% Precision
Random split	10	0.769	0.966	0.208	2,682	0.821
Random split	25	0.769	0.966	0.056	4,082	0.821
Forward split	10	0.362	0.892	0.195	5,359	0.431
Forward split	25	0.362	0.892	0.082	7,579	0.431

Overall, the results establish three core findings. Static evaluation substantially overstates AML effectiveness. Rolling deployment generates large and statistically robust excess regulatory losses relative to a dynamically recalibrated benchmark. Instability in cost-sensitive enforcement thresholds, driven by changes in base rates and score distributions, is a central mechanism underlying regulatory fragility in evolving crypto-asset markets.

Robustness Analysis

To assess the generality of these findings, Appendix B reports three additional robustness exercises. First, we replicate the rolling deployment analysis using XGBoost to determine whether model capacity resolves the observed fragility.

Despite substantially higher predictive accuracy under random evaluation (PR-AUC of 0.978 versus 0.769), forward-split test losses converge across models (7,521 for XGBoost versus 7,579 for logistic regression), and rolling deployment fragility persists, confirming that the result is a property of the decision rule under non-stationarity rather than of any particular model’s predictive limitations (Table B1 B2, Figures B1–B2). Second, we decompose window-level loss ratios using OLS with HAC standard errors to examine the sources of deployment failure. Score dispersion is negatively associated with fragility when measured on contemporaneous test data, but this relationship vanishes when using the training-window dispersion observable at deployment time, indicating that score compression is detectable ex-post but not foreseeable ex-ante (Tables B3 B4 B5, Figures B3–B4). Third, we demonstrate that feasible threshold recalibration fails to close the deployment gap across all tested window lengths (2 to 7 periods). Short recalibration windows amplify estimation noise and worsen loss, while longer windows provide negligible improvement over the static threshold (Table B6, Figures B7–B8). Together, these exercises indicate that deployment fragility is robust to model choice, is not explained by predictable window-level characteristics, and may not be resolved through mechanical threshold updating.

6 Discussion

The results reveal a substantial gap between static machine learning performance and realized regulatory outcomes in crypto asset monitoring. Strong performance under conventional evaluation can co-exist with large and persistent regulatory losses once models are deployed in a changing environment. In other words, high AUC or precision does not guarantee effective enforcement.

This finding connects directly to the concept drift literature, which emphasizes that models trained on historical data may become misaligned when the underlying data-generating process evolves (Widmer and Kubat, 1996; Gama et al., 2014). In cryptocurrency markets characterized by rapid innovation, shifting participation, and evolving transaction patterns, such drift is not merely a statistical inconvenience. Our evidence suggests that it generates economically meaningful increases in enforcement costs when decision rules remain fixed. Prior research documents substantial regime variation in crypto markets driven by speculative trading, regulatory frictions, and changing market structure (Baek and Elbeck, 2015; Baur et al., 2018; Eom, 2021; Biais et al., 2023). We show that such shifts translate into instability in optimal enforcement thresholds and large increases in realized regulatory loss. The economic consequences of regime change are therefore not limited to price dynamics or volatility; they also affect the efficiency of compliance systems.

Methodologically, our findings reinforce broader concerns about model evaluation in finance. A growing literature warns that random train-test splits can produce overly optimistic assessments of model performance when data are temporally dependent or structurally evolving (Bailey et al., 2017; De Prado, 2018). We show that this concern is particularly acute in regulatory settings, where random splits obscure deployment fragility that forward and rolling evaluations reveal clearly. A central contribution of the paper is to highlight threshold instability as a distinct channel of regulatory fragility. Building on cost-sensitive learning (Elkan, 2001), we show that the loss-minimizing threshold varies substantially over time even when the predictive model is held fixed. This instability provides a mechanism through which otherwise stable models can generate inefficient outcomes, echoing work on algorithmic decision systems showing that policy-relevant performance depends on the chosen objective and the decision rule used to translate scores into actions (Kleinberg et al., 2016; Corbett-Davies et al., 2023). More broadly, our findings align with the model risk literature: risk models that appear reliable under backtesting may fail when economic conditions change, generating losses that are foreseeable ex-post but difficult to prevent ex-ante (Danielsson et al., 2016).

From a regulatory design perspective, these results suggest several cautious implications. First, supervisory assessment of AML systems may benefit from incorporating time-respecting evaluation protocols, such as forward-looking or rolling deployment exercises, alongside conventional static metrics. Second, threshold selection may be more appropriately viewed as an ongoing governance decision rather than a one-time technical calibration, particularly in

environments where illicit prevalence and transaction patterns evolve rapidly. Third, evaluating regulatory loss under alternative prevalence or score distribution scenarios may help identify settings in which static enforcement rules are especially fragile. Consistent with industry accounts of transaction monitoring (Oztas et al., 2024), our results suggest that threshold calibration and alert governance are not merely implementation details but first-order determinants of AML effectiveness in fast-changing digital asset environments (Anagnostopoulos, 2018).

Several limitations suggest directions for future research. We focus on a single benchmark dataset and a relatively simple predictive model in order to isolate deployment effects; extending the analysis to alternative architectures or more recent datasets would help assess external validity. In addition, we do not model endogenous behavioral responses by illicit actors to enforcement policies. Strategic adaptation could amplify or mitigate the threshold instability documented here. Finally, incorporating network dynamics more explicitly into the regulatory objective may provide further insight into systemic versus idiosyncratic illicit risk within crypto transaction networks. Addressing these questions would deepen our understanding of regulatory fragility in algorithmic enforcement systems and inform the design of more resilient supervisory frameworks.

7 Conclusion

This paper examines the deployment performance of automated AML systems in evolving cryptocurrency markets and shows that strong static classification metrics substantially overstate real-world regulatory effectiveness. While conventional evaluation suggests high predictive performance, forward-looking and rolling deployment exercises reveal pronounced fragility once enforcement systems operate in non-stationary environments. Optimal enforcement thresholds are highly unstable over time, and when thresholds calibrated on historical data are held fixed during deployment, regulatory losses rise sharply relative to a dynamically recalibrated benchmark. These excess losses are economically meaningful, statistically robust, and persistent across alternative regulatory cost ratios, indicating that deployment fragility is a first-order concern rather than a technical detail.

Our findings clarify that this fragility arises not only from potential declines in predictive accuracy, but from the interaction between temporal non-stationarity and fixed decision rules governing enforcement. Even when the predictive model itself remains unchanged, shifts in illicit prevalence and score distributions render previously optimal thresholds inefficient. By shifting attention from static accuracy metrics to loss-based deployment outcomes, this paper provides a framework for evaluating algorithmic compliance systems in rapidly evolving digital asset markets. More broadly, the results suggest that effective regulatory oversight of automated decision systems requires time-respecting validation, careful governance of enforcement thresholds, and explicit attention to the economic consequences of misclassification.

Declarations

Funding

This research received no external funding. The authors declare that no financial support was provided by public, commercial, or non-profit entities for the conduct of this study.

Conflict of Interest

The authors declare no competing financial or non-financial interests that could have influenced the research reported in this paper.

Ethics Approval

This study does not involve human participants, human subjects data, or experiments requiring ethical approval. All analyses are conducted using publicly available, anonymized transaction-level data.

Data Availability

The Elliptic Bitcoin transaction dataset is publicly available.

Code Availability

All code used to generate the results in this paper is available from the corresponding author upon reasonable request. Replication scripts are designed to reproduce all tables and figures reported in the paper.

References

- Anagnostopoulos, I. (2018). Fintech and regtech: Impact on regulators and banks. *Journal of economics and business*, 100:7–25.
- Baek, C. and Elbeck, M. (2015). Bitcoins as an investment or speculative vehicle? a first look. *Applied Economics Letters*, 22(1):30–34.
- Bailey, D., Borwein, J., Lopez de Prado, M., and Zhu, Q. J. (2017). The probability of backtest overfitting. *The Journal of Computational Finance*, 20(4):39–69.
- Baur, D. G., Hong, K., and Lee, A. D. (2018). Bitcoin: Medium of exchange or speculative assets? *Journal of International Financial Markets, Institutions and Money*, 54:177–189.
- Biais, B., Bisiere, C., Bouvard, M., Casamatta, C., and Menkveld, A. J. (2023). Equilibrium bitcoin pricing. *The Journal of Finance*, 78(2):967–1014.
- Cong, L. W., Li, Y., and Wang, N. (2022). Token-based platform finance. *Journal of Financial Economics*, 144(3):972–991.
- Corbett-Davies, S., Gaebler, J. D., Nilforoshan, H., Shroff, R., and Goel, S. (2023). The measure and mismeasure of fairness. *Journal of Machine Learning Research*, 24(312):1–117.
- Danielsson, J., James, K. R., Valenzuela, M., and Zer, I. (2016). Model risk of risk models. *Journal of Financial Stability*, 23:79–91.
- Davis, J. and Goadrich, M. (2006). The relationship between precision-recall and roc curves. In *Proceedings of the 23rd international conference on Machine learning*, pages 233–240.
- De Prado, M. L. (2018). *Advances in financial machine learning*. John Wiley & Sons.
- Elkan, C. (2001). The foundations of cost-sensitive learning. In *International joint conference on artificial intelligence*, volume 17, pages 973–978. Lawrence Erlbaum Associates Ltd.
- Eom, Y. (2021). Kimchi premium and speculative trading in bitcoin. *Finance Research Letters*, 38:101505.
- Fawcett, T. (2006). An introduction to roc analysis. *Pattern recognition letters*, 27(8):861–874.
- Foley, S., Karlsen, J. R., and Putniņš, T. J. (2019). Sex, drugs, and bitcoin: How much illegal activity is financed through cryptocurrencies? *The review of financial studies*, 32(5):1798–1853.
- Force, F. A. T. (2021). Updated guidance for a risk-based approach to virtual assets and virtual asset service providers. Technical report.
- Gama, J., Žliobaitė, I., Bifet, A., Pechenizkiy, M., and Bouchachia, A. (2014). A survey on concept drift adaptation. *ACM computing surveys (CSUR)*, 46(4):1–37.

- Gandal, N., Hamrick, J., Moore, T., and Oberman, T. (2018). Price manipulation in the bitcoin ecosystem. *Journal of Monetary Economics*, 95:86–96.
- Gu, S., Kelly, B., and Xiu, D. (2020). Empirical asset pricing via machine learning. *The Review of Financial Studies*, 33(5):2223–2273.
- Haider, M., Noreen, T., and Salman, M. (2025). Towards quantum-ready blockchain fraud detection via ensemble graph neural networks. In *2025 7th International Conference on Blockchain Computing and Applications (BCCA)*, pages 898–905. IEEE.
- Hand, D. J. (2009). Measuring classifier performance: a coherent alternative to the area under the roc curve. *Machine learning*, 77(1):103–123.
- Hardjono, T., Lipton, A., and Pentland, A. (2021). Toward a public-key management framework for virtual assets and virtual asset service providers. *The Journal of FinTech*, 1(01):2050001.
- Kelly, B. T., Pruitt, S., and Su, Y. (2019). Characteristics are covariances: A unified model of risk and return. *Journal of Financial Economics*, 134(3):501–524.
- Kleinberg, J., Mullainathan, S., and Raghavan, M. (2016). Inherent trade-offs in the fair determination of risk scores. *arXiv preprint arXiv:1609.05807*.
- Meiklejohn, S., Pomarole, M., Jordan, G., Levchenko, K., McCoy, D., Voelker, G. M., and Savage, S. (2013). A fistful of bitcoins: characterizing payments among men with no names. In *Proceedings of the 2013 conference on Internet measurement conference*, pages 127–140.
- Moreno-Torres, J. G., Raeder, T., Alaiz-Rodríguez, R., Chawla, N. V., and Herrera, F. (2012). A unifying view on dataset shift in classification. *Pattern recognition*, 45(1):521–530.
- Nami, S. and Shajari, M. (2018). Cost-sensitive payment card fraud detection based on dynamic random forest and k-nearest neighbors. *Expert Systems with Applications*, 110:381–392.
- Oztas, B., Cetinkaya, D., Adedoyin, F., Budka, M., Aksu, G., and Dogan, H. (2024). Transaction monitoring in anti-money laundering: A qualitative analysis and points of view from industry. *Future Generation Computer Systems*, 159:161–171.
- Saito, T. and Rehmsmeier, M. (2015). The precision-recall plot is more informative than the roc plot when evaluating binary classifiers on imbalanced datasets. *PloS one*, 10(3):e0118432.
- Schnoering, H. and Vazirgiannis, M. (2025). Bitcoin research with a transaction graph dataset. *Scientific Data*, 12(1):404.
- Sirignano, J. and Cont, R. (2021). Universal features of price formation in financial markets: perspectives from deep learning. In *Machine learning and AI in finance*, pages 5–15. Routledge.
- Weber, M., Domeniconi, G., Chen, J., Weidele, D. K. I., Bellei, C., Robinson, T., and Leiserson, C. E. (2019). Anti-money laundering in bitcoin: Experimenting with graph convolutional networks for financial forensics. *arXiv preprint arXiv:1908.02591*.
- Widmer, G. and Kubat, M. (1996). Learning in the presence of concept drift and hidden contexts. *Machine learning*, 23(1):69–101.

A Supplementary Descriptive Evidence

This appendix reports supplementary descriptive statistics and robustness evidence referenced in the Results section. These materials provide supporting context and inference checks but do not introduce new empirical claims.

A.1 Descriptive Dynamics of Illicit Activity

Table A1 reports labeled transaction counts and illicit prevalence by time-step blocks. Illicit prevalence declines monotonically over time, implying that the base rate relevant for AML enforcement decisions is time-varying.

Table A1: Descriptive Statistics by Time-Step Blocks

Time Step	Observations	Illicit Share	Cumulative Illicit Share
1–10	8,335	0.143	0.143
11–20	10,759	0.117	0.128
21–30	12,864	0.095	0.113
31–40	9,862	0.071	0.103
41–49	4,744	0.053	0.098

A.2 Rolling-Window Summary Statistics

Table A2 reports rolling-window averages of predictive performance, enforcement thresholds, and deployment outcomes for each regulatory cost ratio. These summaries are descriptive and are not used for formal inference.

Table A2: Rolling-Window Summary Statistics

Cost Ratio	Windows	Mean PR-AUC	Mean ROC-AUC	Mean Illicit Share	Mean τ_{train}^*	Mean Loss Ratio	Mean E
$C_{FN}/C_{FP} = 10$	48	0.644	0.920	0.088	0.198	1.966	68
$C_{FN}/C_{FP} = 25$	48	0.644	0.920	0.088	0.085	2.230	15

A.3 Illicit Prevalence in Rolling Test Windows

Figure A1 plots illicit prevalence in the rolling test windows over time. Because cost-sensitive enforcement thresholds depend mechanically on class prevalence and score distributions, these dynamics provide context for the threshold instability documented in the main text.

A.4 Distribution of Deployment Loss Ratios

Figure A2 summarizes the distribution of the deployment loss ratio, defined as deployed regulatory loss divided by oracle loss, pooling across rolling windows and cost ratios.

A.5 Timing of Deployment Loss Ratios

Figures A3 and A4 plot deployment loss ratios over time for each regulatory cost ratio. Loss spikes are episodic rather than uniform, indicating that deployment inefficiency is state-dependent.

A.6 Bootstrap Inference for Excess Regulatory Loss

Table A3 reports moving block bootstrap inference for mean excess regulatory loss under alternative block lengths. Confidence intervals exclude zero across block choices, indicating that excess regulatory loss is statistically robust.

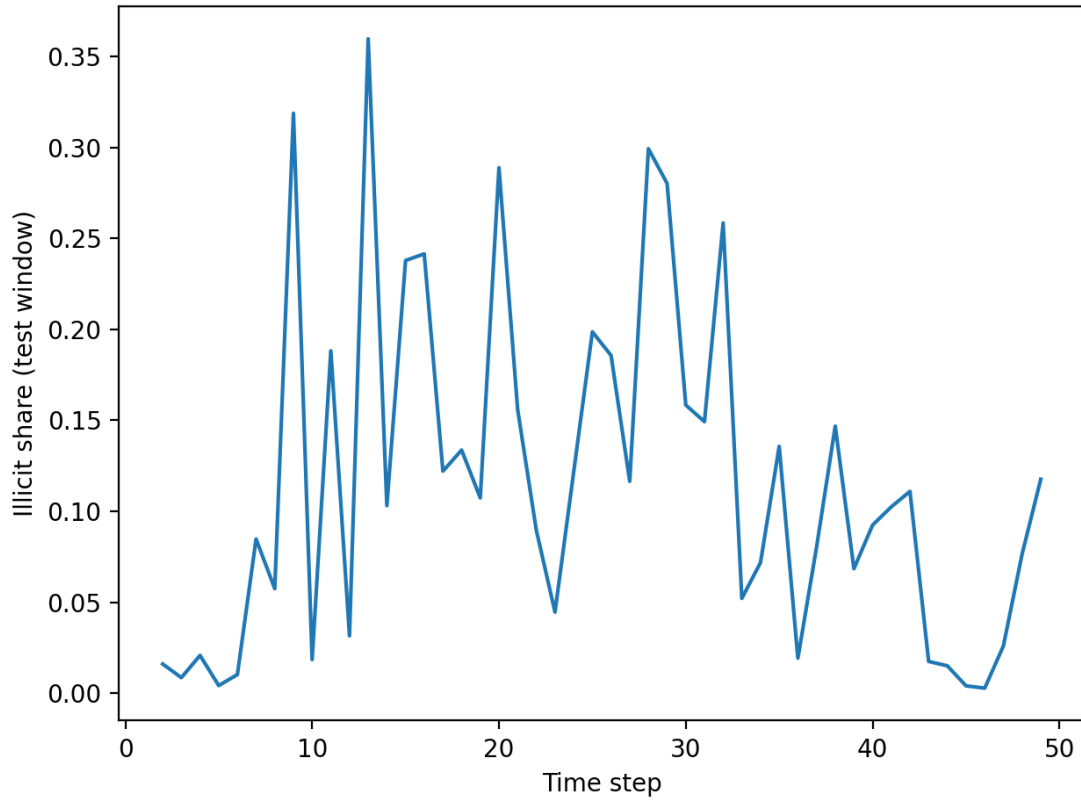


Figure A1: Illicit prevalence over time in rolling test windows.

Table A3: Block Bootstrap Inference for Mean Excess Regulatory Loss

Cost Ratio	Block Length	Mean Excess Loss	SE	CI Low	CI High	Mean Loss Ratio
10	3	68.542	15.252	36.914	96.439	1.966
10	5	68.542	15.373	35.104	94.501	1.966
10	7	68.542	14.600	35.229	91.917	1.966
25	3	154.250	43.549	69.623	237.381	2.230
25	5	154.250	41.915	68.184	230.365	2.230
25	7	154.250	40.253	66.915	222.939	2.230

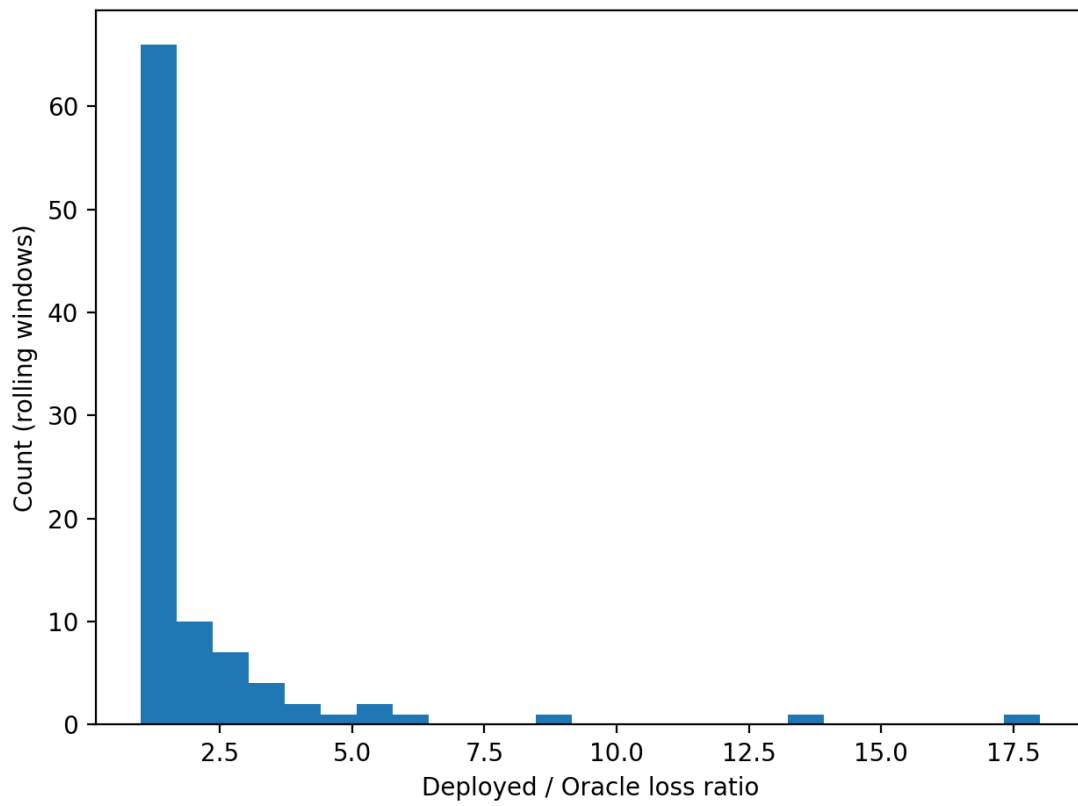


Figure A2: Distribution of deployed-to-oracle regulatory loss ratios across rolling windows.

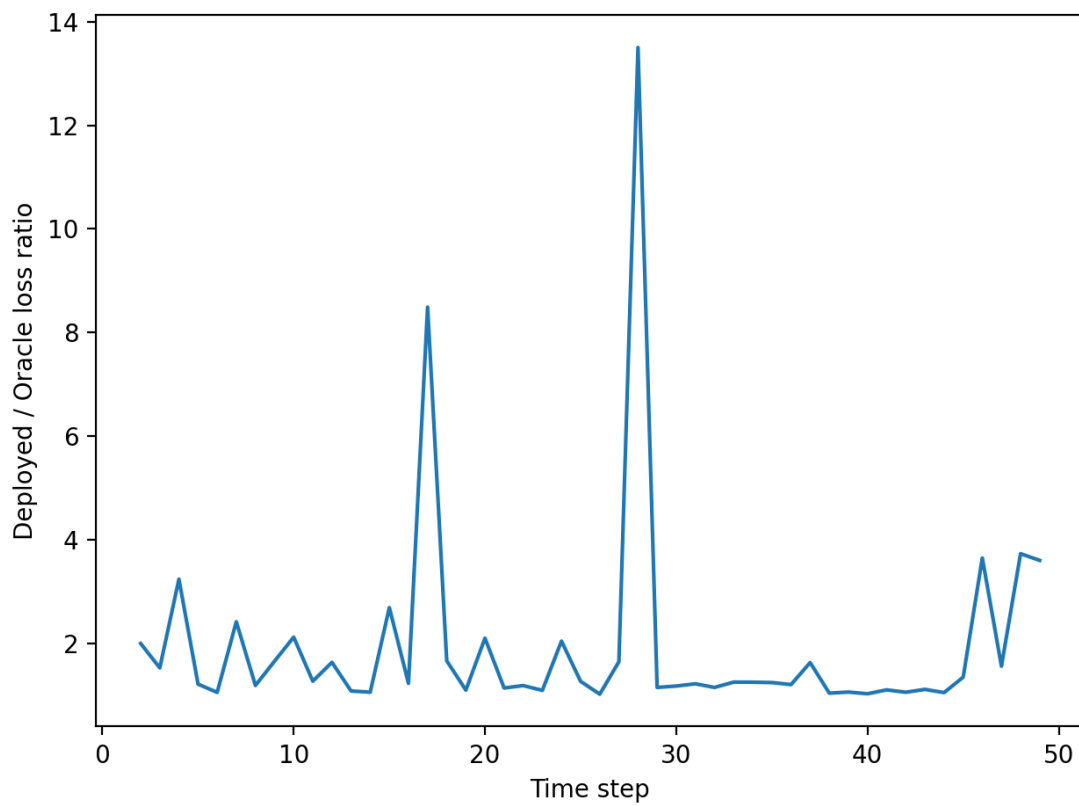


Figure A3: Deployment loss ratio over time ($C_{FN}/C_{FP} = 10$).

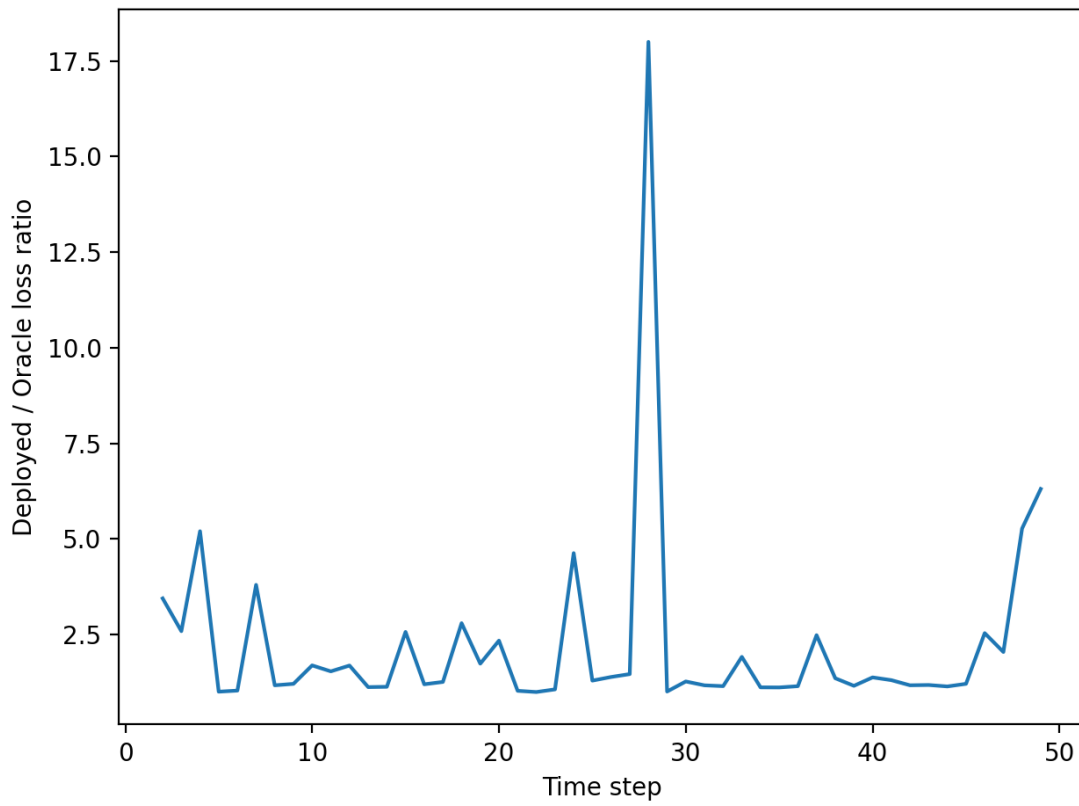


Figure A4: Deployment loss ratio over time ($C_{FN}/C_{FP} = 25$).

B Robustness Analysis

This appendix reports three robustness exercises supplementing the main results. All exercises use the same Elliptic dataset, rolling deployment design, and cost-sensitive loss function described in the main text. The purpose is to assess the sensitivity of the core findings to model choice, mechanism interpretation, and threshold recalibration.

B.1 Alternative Model: XGBoost

Table B1 compares logistic regression and XGBoost under random split, forward split, and rolling deployment. Under random evaluation, XGBoost achieves substantially higher predictive accuracy (PR-AUC = 0.978 versus 0.769; top-1% precision = 1.000 versus 0.821), consistent with its greater model capacity and susceptibility to temporal leakage under non-temporal splits. Once temporal ordering is enforced, forward-split test losses converge sharply across models: at $C_{FN}/C_{FP} = 25$, XGBoost loss is 7,521 versus logistic regression loss of 7,579, a difference of less than one percent despite a gap of 0.427 in PR-AUC. Rolling deployment results confirm this pattern. Mean excess regulatory loss under XGBoost remains large and statistically robust across bootstrap block lengths, and the deployment-to-oracle loss ratio is comparable in magnitude to the logistic regression baseline. These results indicate that deployment fragility is a property of the decision rule under non-stationarity rather than of any particular model’s predictive limitations.

Notably, while XGBoost achieves lower absolute deployed loss than logistic regression, its mean window-level loss ratio is substantially higher (3.67 versus 1.97 at $C_{FN}/C_{FP} = 10$; 7.58 versus 2.23 at $C_{FN}/C_{FP} = 25$), as reported in Table B2. The larger ratio reflects XGBoost’s substantially lower oracle loss rather than worse absolute deployment performance: proportional miscalibration appears larger precisely because the benchmark is more efficient. This indicates that a more capable model can create a larger proportional deployment gap relative to its own oracle benchmark, suggesting that improvements in predictive accuracy do not reduce, and may amplify, the governance consequences of static threshold deployment.

Table B1: Deployment Fragility under Alternative Model Specifications

Model	Protocol	C_{FN}/C_{FP}	PR-AUC	ROC-AUC	τ_{train}^*	Test Loss	Top 1% Prec.
Logistic	Random split	10	0.769	0.966	0.208	2,682	0.821
Logistic	Random split	25	0.769	0.966	0.056	4,082	0.821
Logistic	Forward split	10	0.362	0.892	0.195	5,359	0.431
Logistic	Forward split	25	0.362	0.892	0.082	7,579	0.431
XGBoost	Random split	10	0.978	0.996	0.472	834	1.000
XGBoost	Random split	25	0.978	0.996	0.382	1,410	1.000
XGBoost	Forward split	10	0.789	0.935	0.490	3,488	1.000
XGBoost	Forward split	25	0.789	0.935	0.379	7,521	1.000

Notes: Random split uses a stratified 70/30 split ignoring temporal ordering. Forward split trains on $t \leq 34$ and tests on $t \geq 35$. τ_{train}^* is the cost-minimizing threshold selected on training data. Test loss is $C_{FN} \times FN + C_{FP} \times FP$ on the test set. Top 1% precision is the illicit share among the top 1% of risk-scored transactions.

Figures B1 and B2 illustrate this pattern directly. Deployed loss spikes occur at the same time steps across both models, and XGBoost’s substantially higher PR-AUC (bottom panels) does not translate into meaningfully lower deployment loss (top panels), confirming that fragility is driven by threshold miscalibration rather than predictive accuracy.

B.2 Mechanism Decomposition

Table B3 reports OLS regressions of the log deployment loss ratio on three standardized window-level characteristics: log illicit prevalence, log score dispersion (IQR of predicted probabilities), and prevalence change since training. Standard errors are Newey-West HAC with four lags. Score dispersion is the only consistently significant predictor ($\hat{\beta} = -0.149$, $p = 0.049$ at $C_{FN}/C_{FP} = 10$; $\hat{\beta} = -0.248$, $p = 0.012$ at $C_{FN}/C_{FP} = 25$), with a negative sign

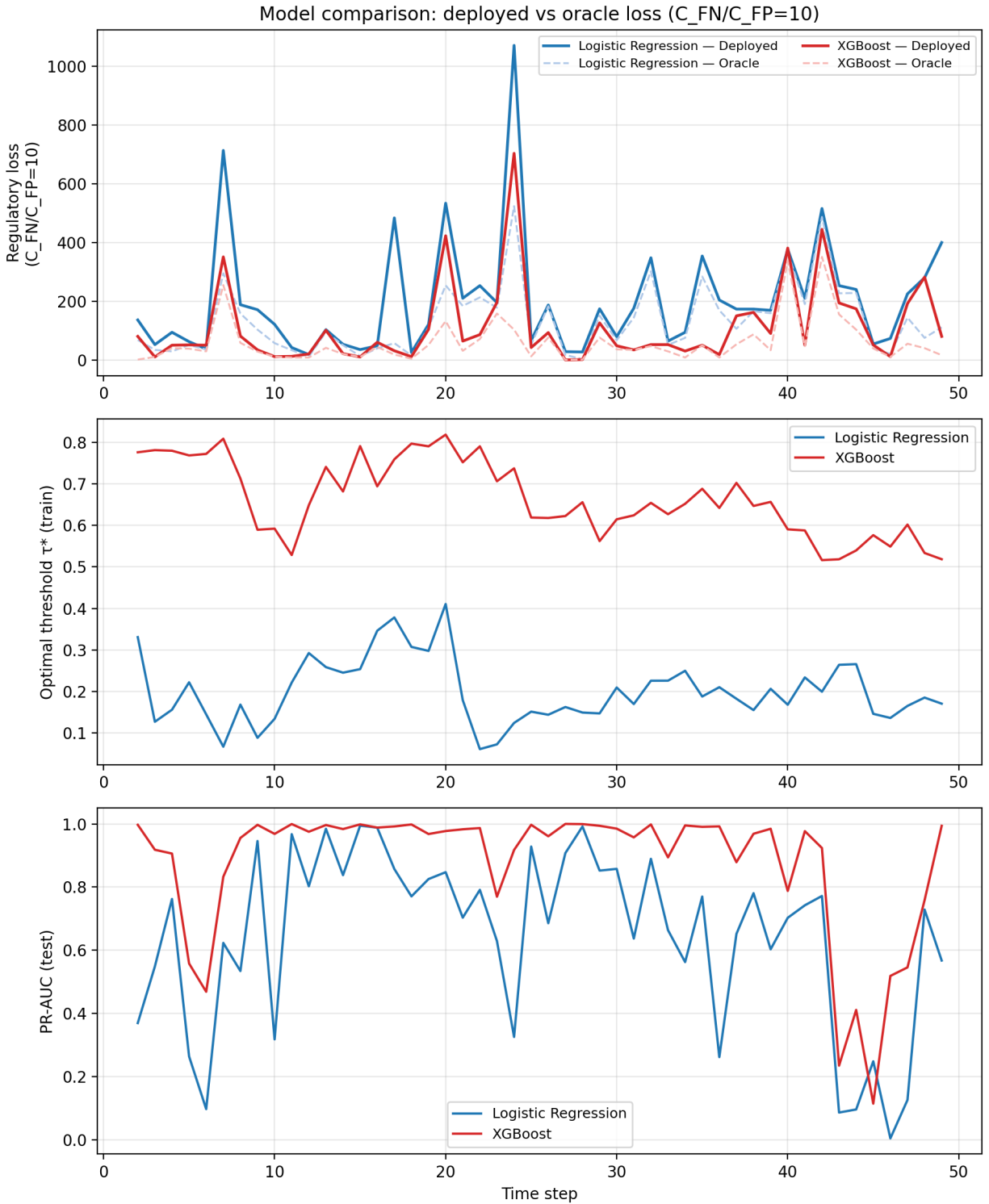


Figure B1: Model comparison: deployed versus oracle regulatory loss, optimal threshold, and PR-AUC over time. $C_{FN}/C_{FP} = 10$. Top panel: deployed loss (solid) and oracle loss (dashed) for logistic regression (blue) and XGBoost (red). Both models exhibit large episodic deployment gaps at the same time steps, despite XGBoost maintaining substantially higher PR-AUC throughout (bottom panel). Middle panel: optimal threshold τ^* from the training window; XGBoost thresholds are higher in level but similarly unstable over time.

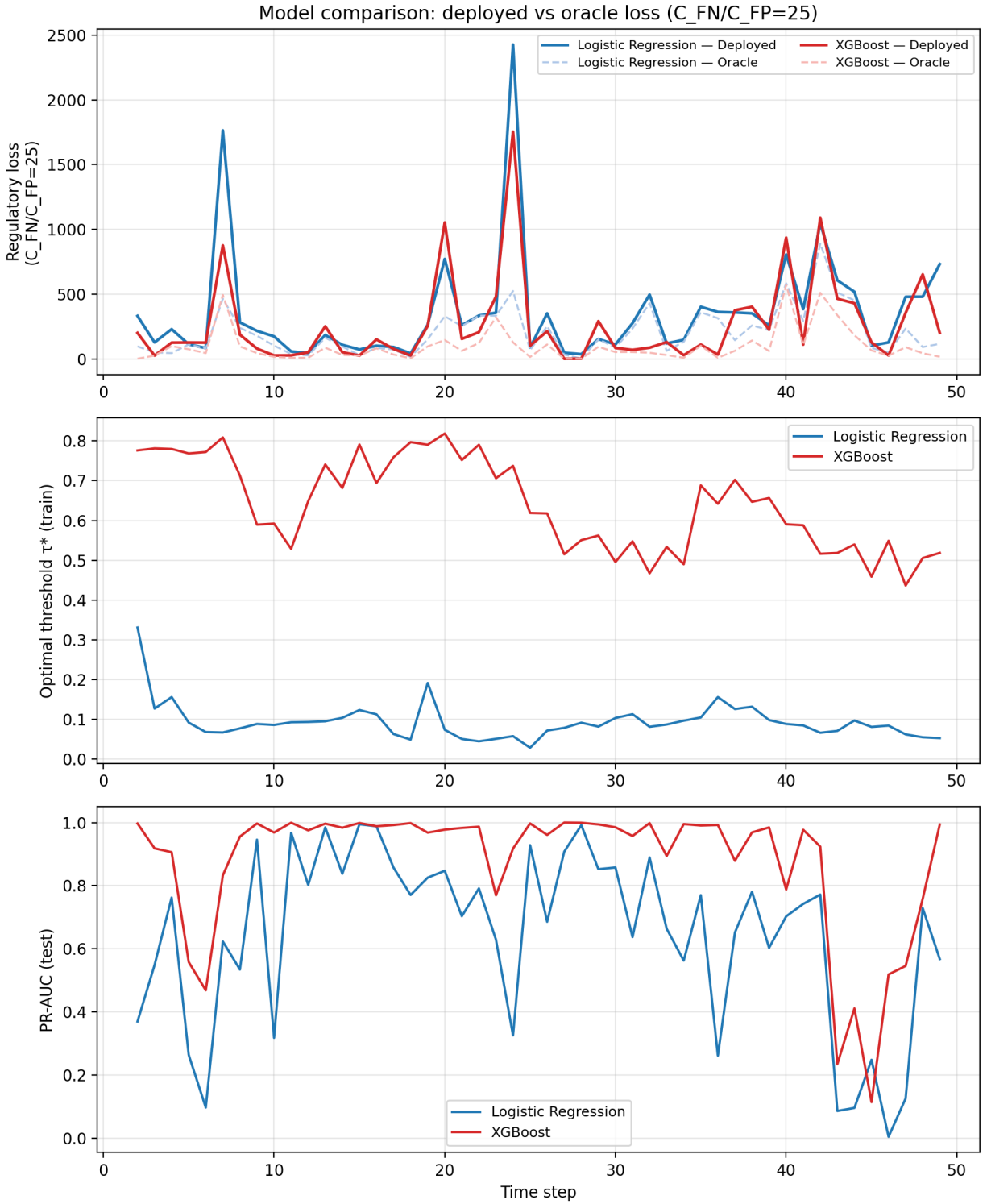


Figure B2: Model comparison: deployed versus oracle regulatory loss, optimal threshold, and PR-AUC over time. $C_{FN}/C_{FP} = 25$. Loss spikes are larger and more persistent than at $C_{FN}/C_{FP} = 10$ for both models. The convergence of deployed loss across models during peak periods, despite persistent PR-AUC differences, illustrates that deployment fragility arises from threshold miscalibration rather than predictive limitations.

Table B2: Rolling Deployment Fragility: Logistic Regression vs XGBoost

Model	C_{FN}/C_{FP}	Mean PR-AUC	Mean Deployed	Mean Oracle	Excess Loss [95% CI]	Loss Ratio [95% CI]
Logistic	10	0.644	202.33	133.79	68.54 [34.96, 95.42]	1.97 [1.41, 2.51]
XGBoost	10	0.872	114.23	61.11	53.13 [26.15, 82.60]	3.67 [1.59, 3.87]
Logistic	25	0.644	359.58	205.33	154.25 [67.04, 230.82]	2.23 [1.53, 2.83]
XGBoost	25	0.872	273.68	101.34	172.34 [96.02, 259.96]	7.58 [2.45, 7.99]

Notes: Rolling deployment results averaged across 48 test windows (47 for XGBoost). Bootstrap 95% confidence intervals use block length 5 and 5,000 replications. Mean loss ratio is deployed loss divided by oracle loss, averaged across windows. XGBoost achieves lower absolute deployed loss than logistic regression but exhibits a substantially higher mean loss ratio, reflecting a larger proportional deployment gap relative to its own oracle benchmark.

indicating that compressed score distributions amplify threshold miscalibration. Illicit prevalence in levels is not a significant predictor, though prevalence change carries positive coefficients that are marginally significant at both cost ratios. The overall R^2 of 0.09–0.14 reflects the episodic nature of loss spikes and is consistent with fragility arising from specific market transitions rather than from stable, predictable window characteristics.

Table B3: OLS Mechanism Decomposition: Log Deployment Loss Ratio

C_{FN}/C_{FP}	Variable	Coef.	HAC SE	t	p
10	Constant	0.458	0.075	6.109	0.000
10	Log illicit prevalence (std)	0.009	0.103	0.083	0.934
10	Log score IQR (std)	-0.149	0.073	-2.026	0.049
10	Prevalence change (std)	0.181	0.099	1.820	0.076
	R^2	0.094	$N = 48$		
25	Constant	0.541	0.084	6.436	0.000
25	Log illicit prevalence (std)	0.063	0.084	0.748	0.458
25	Log score IQR (std)	-0.248	0.095	-2.607	0.012
25	Prevalence change (std)	0.205	0.120	1.712	0.094
	R^2	0.139	$N = 48$		

Notes: Dependent variable is $\log(\text{deployed loss}/\text{oracle loss})$ for each rolling test window. Regressors are standardized to have mean zero and unit standard deviation. IQR is measured on the test-period score distribution (contemporaneous). HAC standard errors use Newey-West with 4 lags.

Table B4 reports a further check replacing test-period IQR with training-period IQR, which is observable at deployment time. The IQR coefficient collapses to insignificance in all specifications ($p > 0.55$ across both cost ratios), and R^2 falls from 0.09–0.14 to approximately 0.05. This indicates that score compression is detectable ex post but not foreseeable ex ante from the information available to regulators at the time enforcement thresholds are set, reinforcing the central conclusion that deployment fragility arises from conditions that cannot be anticipated from the training window.

Table B5 reports mean deployment outcomes by tertile of illicit prevalence. Excess regulatory loss is largest in the middle prevalence tertile (Q2) at both cost ratios, consistent with the regime-transition interpretation: fragility is highest when prevalence is in flux rather than stably high or stably low.

Figures B3 and B4 show partial regression plots for each mechanism variable, controlling for the others. Figures B5 and B6 plot the deployed and oracle thresholds over time with the miscalibration gap shaded, illustrating that the gap is episodic and concentrated in transition periods.

Table B4: IQR Robustness: Test-Period vs Training-Period Score Dispersion

C_{FN}/C_{FP}	Variable	Test IQR (baseline)			Train IQR (robustness)		
		Coef.	HAC SE	p	Coef.	HAC SE	p
10	Log illicit prev. (std)	0.009	0.103	0.934	-0.027	0.164	0.873
10	Log score IQR (std)	-0.149	0.073	0.049	-0.049	0.153	0.751
10	Prevalence change (std)	0.181	0.099	0.076	0.105	0.205	0.610
10	R^2		0.094			0.054	
25	Log illicit prev. (std)	0.063	0.084	0.458	0.011	0.126	0.929
25	Log score IQR (std)	-0.248	0.095	0.012	-0.090	0.150	0.554
25	Prevalence change (std)	0.205	0.120	0.094	0.073	0.189	0.703
25	R^2		0.139			0.051	

Notes: Both specifications include a constant (not reported). Test IQR is measured on the contemporaneous test-window score distribution. Train IQR is measured on the training-window score distribution observable at deployment time. HAC standard errors use Newey-West with 4 lags. $N = 48$ in all specifications.

Table B5: Deployment Loss by Illicit Prevalence Tertile

C_{FN}/C_{FP}	Tertile	N	Mean Illicit Share	Mean τ_{deploy}^*	Mean Loss Ratio	Mean Excess Loss
10	Q1 (low)	16	0.022	0.192	1.642	32.25
10	Q2 (mid)	16	0.100	0.203	2.131	132.44
10	Q3 (high)	16	0.225	0.206	2.123	40.94
25	Q1 (low)	16	0.022	0.108	1.883	78.81
25	Q2 (mid)	16	0.100	0.083	2.379	320.69
25	Q3 (high)	16	0.225	0.090	2.426	63.25

Notes: Windows sorted into tertiles by illicit prevalence in the test period. Mean loss ratio is deployed loss divided by oracle loss, averaged within each tertile. Mean excess loss is deployed minus oracle loss in levels, averaged within each tertile.

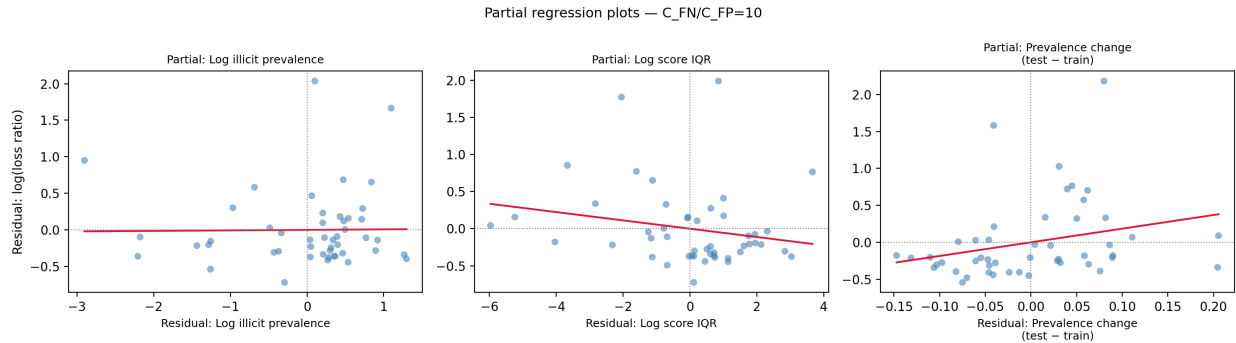


Figure B3: Partial regression plots: log deployment loss ratio on mechanism variables, controlling for the others. $C_{FN}/C_{FP} = 10$. Left panel: log illicit prevalence (no systematic relationship). Centre panel: log score IQR (negative slope, significant at 5%). Right panel: prevalence change since training (positive slope, marginally significant).

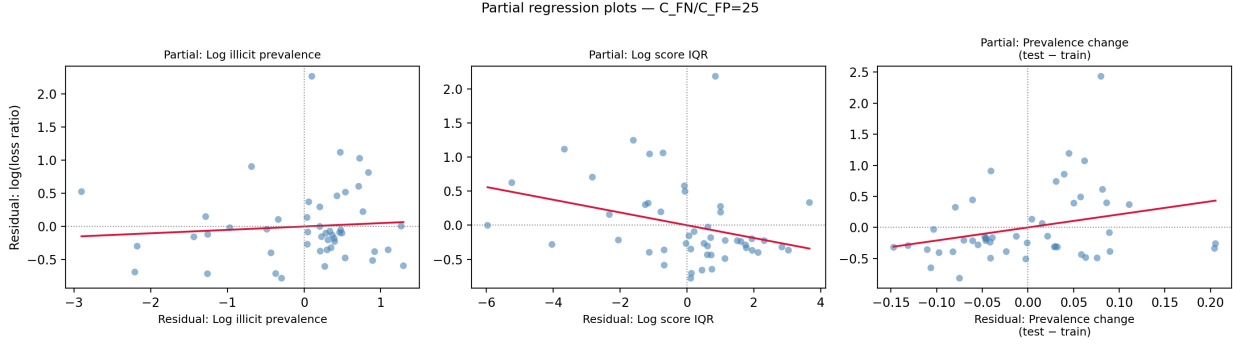


Figure B4: Partial regression plots: log deployment loss ratio on mechanism variables, controlling for the others. $C_{FN}/C_{FP} = 25$. The log score IQR coefficient is more negative and more precisely estimated than at $C_{FN}/C_{FP} = 10$, consistent with heightened sensitivity to score compression under higher enforcement asymmetry.

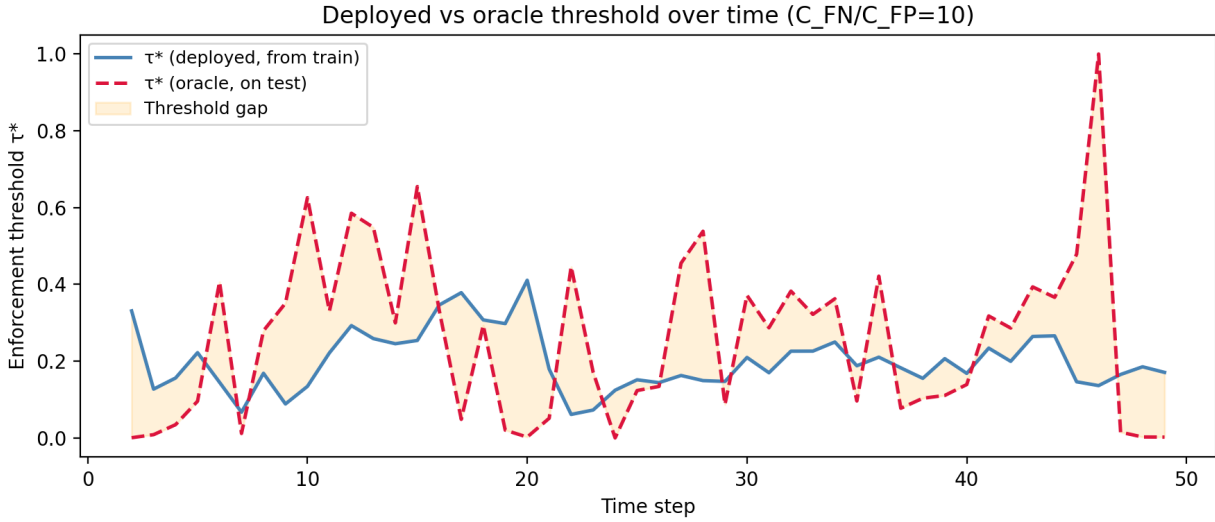


Figure B5: Deployed versus oracle enforcement threshold over time with miscalibration gap shaded. $C_{FN}/C_{FP} = 10$. The oracle threshold (dashed) exhibits large episodic spikes while the deployed threshold (solid) adjusts only slowly, generating the shaded gap.

B.3 Feasible Threshold Recalibration

Table B6 and Figures B7–B8 report results from a feasible recalibration exercise in which the enforcement threshold, but not the underlying model, is re-optimized using a short recent validation window of 2, 3, 5, or 7 time steps prior to each test period.

No recalibration window closes the deployment gap. At $C_{FN}/C_{FP} = 10$, the mean fraction of the gap closed is negative or statistically indistinguishable from zero across all window lengths: window 2 actively worsens loss (fraction closed = -1.37 , 95% CI $[-3.80, -0.05]$); windows 3, 5, and 7 yield fractions of -0.05 , $+0.02$, and -0.05 respectively, with confidence intervals spanning zero in each case. At $C_{FN}/C_{FP} = 25$, results are uniformly negative and statistically significant: fractions closed are -35.4 , -1.76 , -0.38 , and -1.11 for windows 2 through 7 respectively, with confidence intervals excluding zero at block lengths 5 and 7. The asymmetry across cost ratios reflects the greater sensitivity of the loss-minimizing threshold to estimation noise when false negatives are penalized more heavily. Together, these results indicate that the deployment governance problem identified in the main text cannot be resolved through mechanical threshold updating at any recalibration frequency examined here.

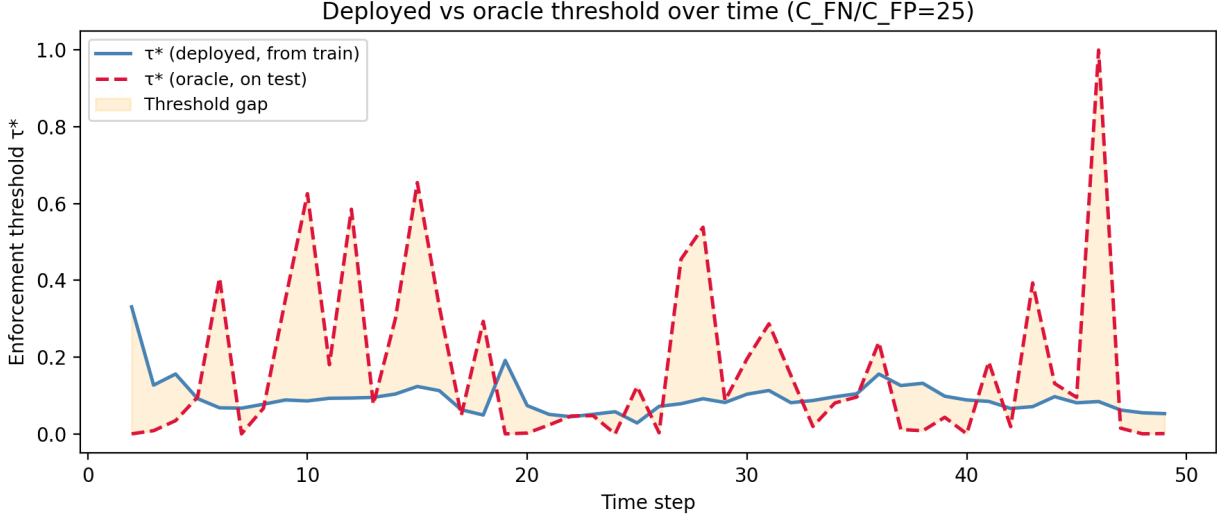


Figure B6: Deployed versus oracle enforcement threshold over time with miscalibration gap shaded. $C_{FN}/C_{FP} = 25$. Threshold spikes are larger and more persistent than at $C_{FN}/C_{FP} = 10$, reflecting the greater sensitivity of the loss-minimizing rule to changes in prevalence and score distributions under higher enforcement asymmetry.

Table B6: Recalibration Window Sensitivity

C_{FN}/C_{FP}	Window	Deployed Loss	Recal Loss	Oracle Loss	Frac. Gap Closed	95% CI
10	2	202.33	222.10	133.79	-1.368	[-3.798, -0.053]
10	3	202.33	198.31	133.79	-0.052	[-0.256, 0.104]
10	5	202.33	197.21	133.79	0.016	[-0.177, 0.153]
10	7	202.33	202.29	133.79	-0.046	[-0.282, 0.110]
25	2	359.58	443.12	205.33	-35.357	[-104.594, -0.193]
25	3	359.58	371.62	205.33	-1.761	[-4.711, -0.235]
25	5	359.58	382.38	205.33	-0.378	[-0.712, -0.144]
25	7	359.58	369.40	205.33	-1.111	[-2.900, -0.137]

Notes: Block bootstrap 95% confidence intervals use block length 5 and 5,000 replications. Deployed loss is regulatory loss under the threshold calibrated on the full rolling training window. Recal loss is regulatory loss under a threshold re-optimized on the most recent w time steps, with the predictive model held fixed. Oracle loss is the infeasible benchmark that re-optimizes on contemporaneous test data. Fraction of gap closed = $1 - (\text{recal loss} - \text{oracle loss}) / (\text{deployed loss} - \text{oracle loss})$.

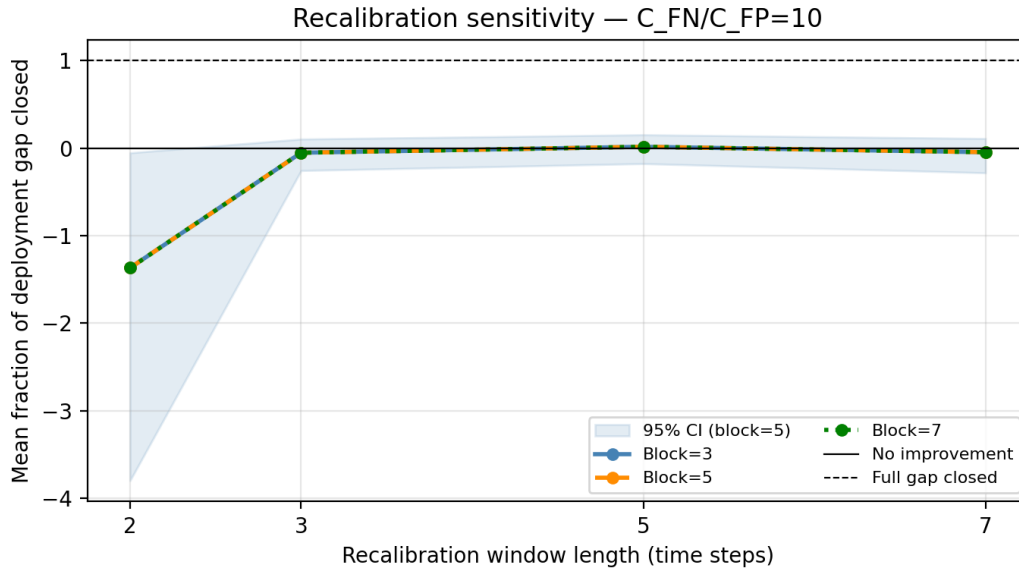


Figure B7: Mean fraction of deployment gap closed by feasible threshold recalibration, across recalibration window lengths 2–7. $C_{FN}/C_{FP} = 10$. Shaded band is the 95% block bootstrap confidence interval (block length 5). The solid horizontal line marks zero (no improvement); the dashed line marks one (full gap closed). All estimates lie at or below zero.

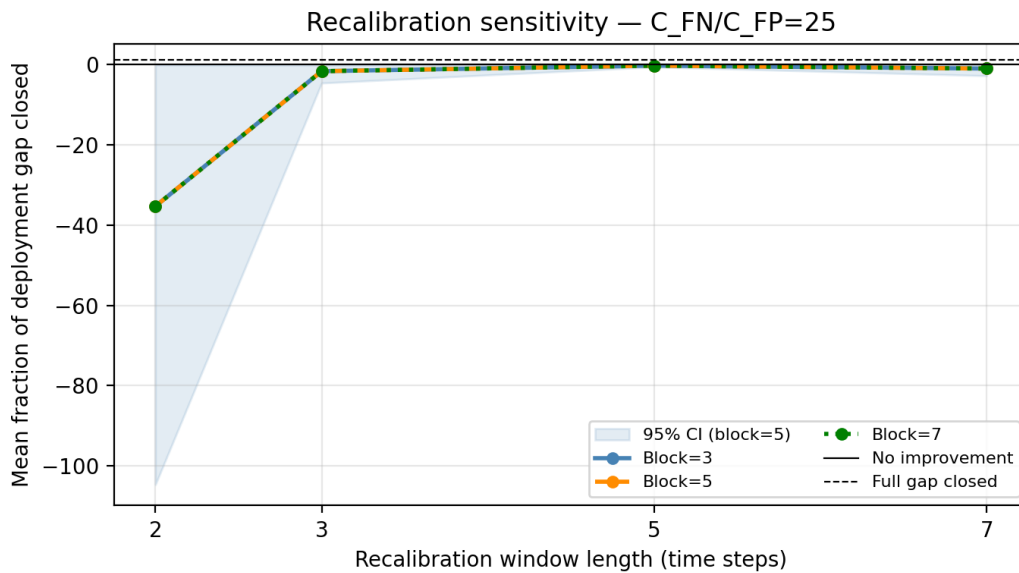


Figure B8: Mean fraction of deployment gap closed by feasible threshold recalibration, across recalibration window lengths 2–7. $C_{FN}/C_{FP} = 25$. The window-2 estimate (−35.4) is suppressed to preserve scale. Confidence intervals exclude zero at windows 3–7, indicating statistically significant worsening relative to the static deployed threshold under high enforcement asymmetry.